Bose-Glass Phases of Ultracold Atoms due to Cavity Backaction

Hessam Habibian,[1,2] André Winter,[1] Simone Paganelli,[2] Heiko Rieger,[1] and Giovanna Morigi[1]

[1]*Theoretische Physik, Universität des Saarlandes, D-66123 Saarbrücken, Germany*

[2]*Departament de Física, Universitat Autònoma de Barcelona, E-08193 Bellaterra, Spain*

(Received 22 June 2012; revised manuscript received 16 November 2012; published 12 February 2013)

We determine the quantum ground-state properties of ultracold bosonic atoms interacting with the mode of a high-finesse resonator. The atoms are confined by an external optical lattice, whose period is incommensurate with the cavity mode wavelength, and are driven by a transverse laser, which is resonant with the cavity mode. While for pointlike atoms photon scattering into the cavity is suppressed, for sufficiently strong lasers quantum fluctuations can support the buildup of an intracavity field, which in turn amplifies quantum fluctuations. The dynamics is described by a Bose-Hubbard model where the coefficients due to the cavity field depend on the atomic density at all lattice sites. Quantum Monte Carlo simulations and mean-field calculations show that, for large parameter regions, cavity backaction forces the atoms into clusters with a checkerboard density distribution. Here, the ground state lacks superfluidity and possesses finite compressibility, typical of a Bose glass. This system constitutes a novel setting where quantum fluctuations give rise to effects usually associated with disorder.

DOI: 10.1103/PhysRevLett.110.075304 PACS numbers: 67.85.−d, 03.75.Hh, 05.30.Jp, 32.80.Qk

Bragg diffraction is a manifestation of the wave properties of light and provides a criterion for the existence of long-range order in the scattering medium [1]. Bragg diffraction of light by atoms in optical lattices was measured for various geometries and settings, from gratings of laser-cooled atoms [2–5] to ultracold bosons in the Mott-insulator (MI) phase [6]. In most of these setups, the mechanical effect of the scattered light on the density distribution of the atomic medium is negligible, while photon recoil can give rise to visible effects in the spectrum of the diffracted light [7].

Recent work proposed to use high-finesse optical resonators to enhance light scattering into one spatial direction so as to reveal properties of the medium's quantum state by measuring the light at the cavity output [7,8]. These proposals assume that backaction of the cavity field on the atoms can be discarded. Such an assumption is, however, not valid in the regime considered in Refs. [9–14]: Here, the strong coupling between cavity and atoms can induce the formation of stable Bragg gratings in cold [9,10] and ultracold atomic gases [11–14] that coherently scatter light from a transverse laser into the cavity mode. This phenomenon occurs when the intensity of the pump exceeds a certain threshold [10,11,13,15]. At ultralow temperatures the self-organized medium is a supersolid [13], while for larger pump intensities incompressible phases are expected [16].

Let now the atoms be inside a high-finesse standing-wave cavity and form a periodic structure, like the one sketched in Fig. 1, whose period $\lambda_0/2$ is incommensurate with the cavity-mode wavelength λ. If the atoms are pointlike scatterers, or deep in a MI phase of the external potential, there is no coherent scattering from a transverse laser into the cavity mode [8,17]. Quantum fluctuations, however, will induce scattering into the cavity, thus the creation of a weak potential with periodicity λ which is incommensurate with λ_0. In this Letter, we derive a Bose-Hubbard model for the system in Fig. 1 and show that cavity backaction gives rise to an additional term in the atomic energy which depends on the density at all lattice sites. Even for weak probe fields this results in the formation of patterns which maximize scattering into the cavity mode and can exhibit finite compressibility with no long-range coherence. This feature, typical of disordered systems, corresponds to a Bose-glass phase for sufficiently deep potentials [18–21] and here emerges due to the nonlocal quantum potential of the cavity field. Our work extends studies predicting glassiness in multimode cavities [22,23].

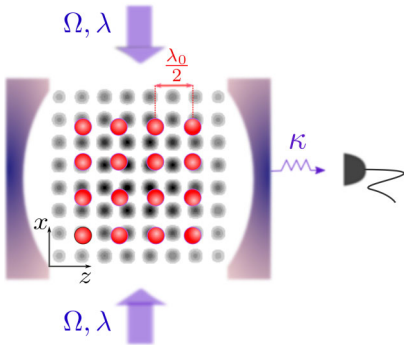

FIG. 1 (color online). Ultracold atoms are tightly confined by an optical lattice of periodicity $\lambda_0/2$. They are driven by a weak transverse laser at Rabi frequency Ω and strongly coupled to the mode of a standing-wave cavity both at wavelength λ. Since λ and λ_0 are incommensurate, light is scattered into the cavity mode because of quantum fluctuations. It then gives rise to an incommensurate long-range interaction between the atoms which modifies the density distribution.

To analyze the quantum dynamics of the atom-cavity system, we assume that the atomic motion is confined to the x-z plane, where $\mathbf{r} = (x, z)$ is the atomic position. The laser and cavity mode have wave vector $\mathbf{k}_L = k\hat{x}$ and $\mathbf{k}_{\rm cav} = k\hat{z}$, respectively, and polarizations such that only a two-level dipolar transition at frequency ω_0 is driven. Moreover, the scattering processes are coherent, which is warranted when the detuning $\Delta_a = \omega_L - \omega_0$ of the pump frequency ω_L from ω_0 has modulus much larger than the transition linewidth, the strength of the atom-photon coupling, and $|\delta_c|$, with $\delta_c = \omega_L - \omega_c$ the detuning of the pump from the mode frequency [13,16]. Let $\hat{a}$ and $\hat{a}^\dagger$ be the operators annihilating and creating a cavity photon and $\hat{\psi}(\mathbf{r})$ be the atomic field operator with $[\hat{\psi}(\mathbf{r}), \hat{\psi}^\dagger(\mathbf{r}')] = \delta^{(2)}(\mathbf{r} - \mathbf{r}')$. In the reference frame rotating at frequency ω_L, the Hamiltonian governing the coherent dynamics reads $\hat{H} = -\hbar\delta_c\hat{a}^\dagger\hat{a} + \hat{H}_a + \hat{H}_i$, with $\hat{H}_{\ell=a,i} = \int d\mathbf{r}\,\hat{\psi}^\dagger(\mathbf{r})\hat{\mathcal{H}}_\ell(\mathbf{r})\hat{\psi}(\mathbf{r})$. Here, $\hat{\mathcal{H}}_a(\mathbf{r}) = \frac{\hbar^2}{2m}\nabla^2 + V_0(\mathbf{r}) + \mathcal{G}_s\hat{n}(\mathbf{r}) + V_1\cos^2(kx)$ describes the atom dynamics in the absence of the resonator and in the presence of the external periodic potential $V_0(\mathbf{r}) = V_t\{\cos^2(k_0 z) + \beta\cos^2(k_0 x)\}$ with wave number k_0, depth V_t along z, and aspect ratio β. Moreover, $\hat{n}(\mathbf{r}) = \hat{\psi}^\dagger(\mathbf{r})\hat{\psi}(\mathbf{r})$ is the atomic density operator, $\mathcal{G}_s$ is the strength of s-wave collisions, and $V_1 = \hbar\Omega^2/\Delta_a$ such that $|V_1|$ is the depth of the dynamical Stark shift induced by the transverse standing-wave laser at Rabi frequency Ω. The atom-cavity coupling reads

$$\hat{\mathcal{H}}_i(\mathbf{r}) = \hbar U_0\cos^2(kz)\hat{a}^\dagger\hat{a} + \hbar S_0\cos(kx)\cos(kz)(\hat{a}^\dagger + \hat{a}), \tag{1}$$

where $U_0 = g_0^2/\Delta_a$ is the dynamical Stark shift per cavity photon and g_0 is the vacuum Rabi frequency at a cavity-field maximum [16,24]. The frequency $S_0 = g_0\Omega/\Delta_a$ is the amplitude of scattering a laser photon into the cavity mode by one atom. The corresponding term describes the coherent pump on the cavity field via scattering by the atoms and depends on the atomic positions within the field. It gives rise to a large intracavity-photon number $n_{\rm cav}$ when the atoms form a Bragg grating with periodicity $2\pi/k$. This would correspond to choosing $k = k_0$: $n_{\rm cav}$ then depends on the balance between the superradiant scattering strength $S_0 N$ and the rate of cavity loss κ. On the contrary, in this work we take k and k_0 to be incommensurate and analyze the effect of cavity backaction when the atoms are tightly confined by the potential $V_0(\mathbf{r})$ and weakly pumped by the transverse laser.

We now sketch the derivation of the Bose-Hubbard Hamiltonian for the atom dynamics. We first assume that in the time scale Δt the atomic motion does not significantly evolve while the cavity field has reached a local steady state, $\int_t^{t+\Delta t}\hat{a}(\tau)d\tau/\Delta t \approx \hat{a}_{\rm st}$, where the time evolution is governed by the Heisenberg-Langevin equation $\dot{\hat{a}} = [\hat{a}, \hat{H}]/i\hbar - \kappa\hat{a} + \sqrt{2\kappa}\hat{a}_{\rm in}(t)$, with $\hat{a}_{\rm in}(t)$ the input noise, $[\hat{a}_{\rm in}(t), \hat{a}_{\rm in}^\dagger(t')] = \delta(t - t')$. The conditions for a time-scale separation are set by the inequality $|\delta_c + i\kappa|\Delta t \gg 1$ and by the assumption that coupling strengths between atoms and fields are much smaller than $1/\Delta t$ [25]. The stationary field reads

$$\hat{a}_{\rm st} = \frac{S_0\hat{\mathcal{Z}}}{(\delta_c - U_0\hat{\mathcal{Y}}) + i\kappa} + \frac{i\sqrt{2\kappa}\hat{\bar{a}}_{\rm in}}{(\delta_c - U_0\hat{\mathcal{Y}}) + i\kappa}, \tag{2}$$

with $\hat{\bar{a}}_{\rm in}$ the input noise averaged over Δt. Here, $\hat{\mathcal{Y}} = \int d^2\mathbf{r}\cos^2(kz)\hat{n}(\mathbf{r})$ and $\hat{\mathcal{Z}} = \int d^2\mathbf{r}\cos(kz)\cos(kx)\hat{n}(\mathbf{r})$ describe the shift of the cavity resonance and coherent scattering amplitude, respectively, due to the atomic density distributions. The noise term can be neglected when the mean intracavity-photon number is larger than its fluctuations, i.e., $|S_0\langle\hat{\mathcal{Z}}\rangle| \gg \kappa$. In this limit, one can monitor the state of the atoms via the field at the cavity output, $\hat{a}_{\rm out} = \sqrt{2\kappa}\hat{a}_{\rm st} - \hat{a}_{\rm in}$ [17]. Using Eq. (2) for $\hat{a}$ in Eq. (1) leads to an effective Hamiltonian, from which we derive a Bose-Hubbard model assuming that the atoms are tightly trapped in the lowest band of $V_0(\mathbf{r})$. We use $\hat{\psi}(\mathbf{r}) = \sum_i w_i(\mathbf{r})\hat{b}_i$, with $w_i(\mathbf{r})$ the Wannier function centered at the minimum $\mathbf{r}_\mathbf{i}$ of potential $V_0(\mathbf{r})$ and $\hat{b}_i$ the bosonic operator annihilating a particle at $\mathbf{r}_\mathbf{i}$. We apply the thermodynamic limit where $S_0 = s_0/\sqrt{K}$ and $U_0 = u_0/K$ with K the number of lattice sites [16] and obtain the Bose-Hubbard Hamiltonian

$$\hat{\mathcal{H}}_{\rm BH} = \sum_{i=1}^{K}\left(\frac{U}{2}\hat{n}_i(\hat{n}_i - 1) - \hat{\mu}_i\hat{n}_i - \sum_{\langle j,i\rangle}\hat{t}_i(\hat{b}_i^\dagger\hat{b}_j + \text{H.c.})\right), \tag{3}$$

with $\hat{n}_i = \hat{b}_i^\dagger\hat{b}_i$ the on site atomic density, $U = \mathcal{G}_s\int d^2\mathbf{r}[w_i(\mathbf{r})]^4$ the on site interaction strength, $\hat{\mu}_i$ the site-dependent chemical potential, $\hat{t}_i$ the tunneling coefficient, and $\langle j, i\rangle$ the sum over nearest neighbors. Here, $\hat{\mu}_i = \mu^{(0)} + \delta\hat{\mu}_i$, $\hat{t}_i = t^{(0)} + \delta\hat{t}_i$, where $\mu^{(0)} = -E_0 - V_t X_0$ and $t^{(0)} = -E_1 - V_t X_1$ are constant over the lattice, with $E_{s=0,1} = -\hbar^2/(2m)\int d^2\mathbf{r}\,w_i(\mathbf{r})\nabla^2 w_{i+s}(\mathbf{r})$ and $X_{s=0,1} = \int d^2\mathbf{r}\{\cos^2(k_0 z) + \beta\cos^2(k_0 x)\}w_i(\mathbf{r})w_{i+s}(\mathbf{r})$. The terms $\delta\hat{\mu}_i$ and $\delta\hat{t}_i$ are due to the pump and cavity incommensurate potentials and vanish when the pump laser is off, $\Omega = 0$. In this limit the model reduces to the regular Bose-Hubbard model exhibiting a MI-superfluid (SF) transition as a function of the parameters μ and t [18]. When $\Omega \neq 0$, still $t_i = t^{(0)}$ since $\delta\hat{t}_i$ is negligible, while

$$\delta\hat{\mu}_i = -V_1 J_0^{(i)} - \hbar\frac{s_0^2}{\hat{\delta}_{\rm eff}^2 + \kappa^2}\hat{\Phi}(2\hat{\delta}_{\rm eff}Z_0^{(i)} + u_0\hat{\Phi}Y_0^{(i)}). \tag{4}$$

Here, $J_0^{(i)} = \int d^2\mathbf{r}\cos^2(kx)w_i(\mathbf{r})^2$ scales the strength of the classical transverse potential due to the laser and is constant for the sites with the same x value, $Z_0^{(i)} = \int d^2\mathbf{r}\cos(kx)\cos(kz)w_i(\mathbf{r})^2$ and $Y_0^{(i)} = \int d^2\mathbf{r}\cos^2(kz)\times w_i(\mathbf{r})^2$ are due the cavity field, whereas $\hat{\delta}_{\rm eff} = \delta_c - u_0\sum_i Y_0^{(i)}\hat{n}_i/K$ is an operator and accounts for the frequency

shift due to the atoms [24,26]. Remarkably, the cavity effects are scaled by the operator

$$\hat{\Phi} = \sum_{i=1}^{K} Z_0^{(i)} \hat{n}_i / K, \tag{5}$$

which originates from the long-range interaction mediated by the cavity field and is related to the mean intracavity photon number since $n_{\mathrm{cav}} \propto \langle \hat{\Phi}^2 \rangle$. Its mean value vanishes when the atomic gas forms a MI state: $\langle \hat{\Phi} \rangle_{\mathrm{MI}} \propto \sum_i Z_0^{(i)} = 0$, since there is no coherent scattering into the cavity mode. Also deep in the SF phase $\langle \hat{\Phi} \rangle_{\mathrm{SF}} \to 0$. Close to the MI-SF phase transition, however, fluctuations in the atomic density lead to finite values of $\langle \hat{\Phi} \rangle$ and, hence, to a finite intracavity photon number. The dependence of the chemical potential on the operator $\hat{\Phi}$ is a peculiar property of our model that distinguishes it from the case of a bichromatic optical lattice [20,21], where the strength of the incommensurate potential is independent of the phase of the ultracold atomic gas.

We first analyze the ground state of the Bose-Hubbard Hamiltonian, Eq. (3), when the system can be reduced to a one-dimensional (1D) lattice along the cavity axis ($\beta \gg 1$). In 1D the effect of the transverse potential [first term in Eq. (4)] is a constant shift which can be reabsorbed in the chemical potential. Figure 2(a) displays the phase diagram in the μ-t plane evaluated by means of a quantum Monte Carlo calculation [27]. The compressibility is determined by using $\chi = \frac{\partial \bar{n}}{\partial \mu}$, with $\bar{n} = \sum_i \langle \hat{n}_i \rangle / K$ the mean density, while the SF density is obtained by extrapolating the Fourier transform of the pseudo current-current correlation function $J(\omega)$ [27] to zero frequency [see the inset in Fig. 2(b)]. The gray regions indicate the MI states at densities $\bar{n} = 1$, 2, and the blue regions a compressible phase where the SF density vanishes, while outside the phase is SF. The effect of cavity backaction is evident at low tunneling, where $\langle \hat{\Phi} \rangle \neq 0$: Here the size of the MI regions is reduced. At larger tunneling a direct MI-SF transition occurs, and the MI-SF phase boundary merges with the one found for $s_0 = 0$: In fact, for larger quantum fluctuations $\langle \hat{\Phi} \rangle \to 0$ in the thermodynamic limit. This feature is strikingly different from the situation in which the incommensurate potential is classical [30,31]: There, the MI lobes shrink at all values of t with respect to the pure case. The atomic density and corresponding value of $\langle \hat{\Phi} \rangle$ are displayed in Figs. 2(b) and 2(c) as a function of μ for different values of the transverse laser intensity (thus s_0): The incommensurate potential builds in the blue region of the diagram, which we label by BG, where the number of intracavity photons does not vanish. Figure 2(d) displays the local density distribution $\langle \hat{n}_i \rangle$ and the local density fluctuations in the BG region: The density oscillates in a quasiperiodic way over clusters in which the atoms scatter in phase into the cavity mode. The fluctuations are larger at the points where $Z_0^{(i)}$, which oscillates at the cavity mode wavelength, becomes out of phase with the trapping potential. Note that by means of this rearrangement the fields emitted by each clusters add up coherently: In this way the density distribution maximizes scattering into the cavity mode. This distribution is reminiscent of a density wave, which is characterized by a zero order parameter and nonvanishing compressibility. We denote the corresponding region by BG, which stands for Bose glass, using the terminology applied in Refs. [30,31] to similar density distributions found in the bichromatic Bose-Hubbard model.

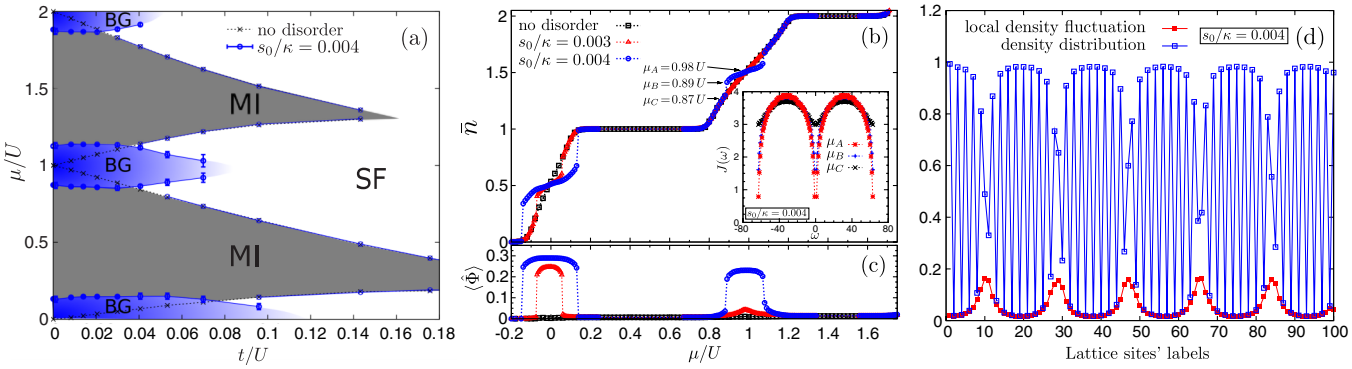

FIG. 2 (color online). Results of quantum Monte Carlo simulations for a 1D lattice ($\beta \gg 1$) with 100 sites and periodic boundary conditions. (a) Phase diagram in the μ-t plane for $s_0 = 0.004\kappa$. The gray regions indicate incompressible phases at density $\bar{n} = 1$, 2, the blue region the gapless phases with vanishing SF density. The dotted lines indicate the incompressible phases in the absence of the pump laser ($s_0 = 0$) [27]. (b) Linear density $\bar{n}$ and (c) $\langle \hat{\Phi} \rangle$ versus μ for $t = 0.053U$ and $s_0/\kappa = 0.003$ (triangles), $s_0/\kappa = 0.004$ (circles), and $s_0 = 0$ (squares): The number of photons is different from zero for the parameters of the BG regions in (a). Inset: Fourier transform of the pseudo current-current correlation function $J(\omega)$ [27] for the parameters indicated by the arrows in (b). (d) Local density distribution $\langle \hat{n}_i \rangle$ (empty points joined by the blue curve) and local density fluctuations $\langle \hat{n}_i^2 \rangle - \langle \hat{n}_i \rangle^2$ (filled points joined by the red curve) as a function of the site for $\mu = 0$ and $s_0 = 0.004\kappa$. The values of $s_0 = \sqrt{K}\Omega g_0/\Delta_a$ are found from $g_0/2\pi = 14.1$ MHz, $\kappa/2\pi = 1.3$ MHz, and detunings about $\Delta_a/2\pi = 58$ GHz [13]. The other parameters are $\delta_c = -5\kappa$, $k/k_0 = 785/830$ as in Ref. [13], and $\mathcal{G}_s$ was taken from Ref. [37].

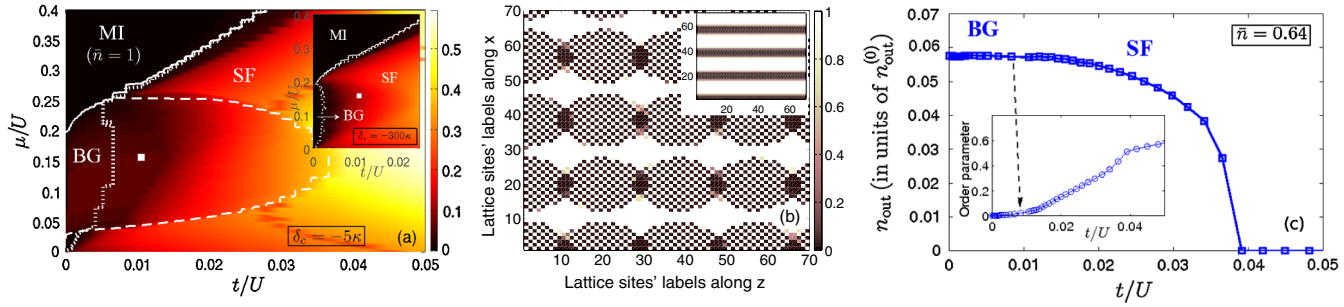

FIG. 3 (color online). Results of a mean-field calculation for a 2D lattice with 70×70 sites and periodic boundary conditions. (a) Order parameter Θ in the μ-t plane when $s_0 = 0.15\kappa$ ($\delta_c = -5\kappa$). Inset: Phase diagram when cavity backaction is negligible ($\delta_c = -300\kappa$). The dotted and solid curves delineate the regions with a small, arbitrarily chosen threshold (here 0.02) for Θ and the density fluctuations, respectively, while inside the dashed curve the number of photons is at least 100 times larger than outside. The localized regions at smaller Θ deep in the SF phase are due to the transverse incommensurate pump. (b) Local density distribution $\langle \hat{n}_i \rangle$ at $\mu = 0.156U$ and $t = 0.01U$ [point in (a) at $\bar{n} = 0.64$]. Inset: Corresponding density distribution in the μ-t plane for $\delta_c = -300\kappa$ (here $\bar{n} = 0.625$). (c) Photon emission rate at the cavity output, $n_{out} = \langle a_{out}^\dagger a_{out} \rangle$, as a function of t for $\bar{n} = 0.64$ and in units of $n_{out}^{(0)} = \kappa n_{cav}^{(max)}$. Inset: Corresponding order parameter. Here, $n_{cav}^{(max)} = s_0^2 K/(\hat{\delta}_{eff}^2 + \kappa^2)$ is the intracavity photon number when all atoms scatter in phase into the cavity mode, $s_0 = 0.15\kappa$ is consistent with the parameters of Ref. [13] for 300×300 sites, and $\mathcal{G}_s$ was taken from Ref. [38].

The two-dimensional (2D) case is studied by means of a mean-field calculation [18,32] for a pumping strength s_0 such that $\max\{|\langle \delta \hat{\mu}_i \rangle|\} < U$. Here, the transverse laser determines the transverse density distribution even when the cavity field is zero. In this case the MI lobes at $t = 0$ shrink due to the classical incommensurate field. Because of the classical potential, in general no direct MI-SF transition is expected [33]. Figure 3(a) displays the order parameter, $\Theta = \sum_i \langle \hat{b}_i \rangle / K$, in the μ-t plane and for density $\bar{n} \leq 1$. The solid curve indicates where the gap in the spectrum is different from zero, corresponding to vanishing density fluctuations $\Delta\varrho = (\overline{n^2} - \bar{n}^2)^{1/2}$, for $\overline{n^2} = \sum_i \langle \hat{n}_i^2 \rangle / K$ [34,35]. The dashed line separates the parameter region where the number of intracavity photons is at least 2 orders of magnitude larger than outside. For comparison the diagram for $n_{cav} \simeq 0$ is reported in the inset. A larger region with vanishing Θ appears when the atoms are strongly coupled to the cavity. The analysis of the corresponding density distribution shows a peculiar behavior. Figure 3(b) displays the local density for $\delta_c = -5\kappa$ for the parameters indicated by the point in (a): The coupling with the resonator induces the formation of clusters with checkerboard density distribution, where the atoms scatter in phase into the cavity mode. At the border of the clusters, the density fluctuates, so as to allow the fields scattered by each cluster to interfere constructively. The inset shows that the clustering disappears when cavity backaction is negligible. In this latter case the field at the cavity output is zero, while when the effect of cavity backaction is relevant it has a finite intensity for a finite range of values of t [Fig. 3(c)]. When the tunneling rate is instead sufficiently large, there is no clustering and the atomic density becomes uniform along the cavity axis. Thus, the competition between the mechanical effects of the cavity field and quantum fluctuations leads to the creation of these clusters, which exhibit properties ranging from a BG to a strongly correlated SF and then disappear when tunneling becomes large.

In conclusion, we predicted an instance of self-organization of a quantum gas in a high-finesse resonator that is triggered by quantum fluctuations of the atomic motion and could be observed in existing experimental setups [13,36].

We acknowledge discussions with A. Niederle, G. De Chiara, S. Fernández-Vidal, M. Lewenstein, and H. Ritsch and support by the European Commission (IP AQUTE), the Spanish Ministerio de Ciencia y Innovación (QOIT: Consolider-Ingenio 2010; FPI; Juan de la Cierva), the Generalitat de Catalunya (SGR2009:00343), and the German Research Foundation.

[1] R. Lifshitz, Z. Kristallogr. **222**, 313 (2007).
[2] G. Birkl, M. Gatzke, I. H. Deutsch, S. L. Rolston, and W. D. Phillips, Phys. Rev. Lett. **75**, 2823 (1995).
[3] M. Weidemüller, A. Hemmerich, A. Görlitz, T. Esslinger, and T. W. Hänsch, Phys. Rev. Lett. **75**, 4583 (1995); M. Weidemüller, A. Görlitz, T. W. Hänsch, and A. Hemmerich, Phys. Rev. A **58**, 4647 (1998).
[4] S. Slama, C. von Cube, B. Deh, A. Ludewig, C. Zimmermann, and Ph. W. Courteille, Phys. Rev. Lett. **94**, 193901 (2005).
[5] S. Slama, C. von Cube, M. Kohler, C. Zimmermann, and Ph. W. Courteille, Phys. Rev. A **73**, 023424 (2006).
[6] C. Weitenberg, P. Schauß, T. Fukuhara, M. Cheneau, M. Endres, I. Bloch, and S. Kuhr, Phys. Rev. Lett. **106**, 215301 (2011).
[7] S. Rist, C. Menotti, and G. Morigi, Phys. Rev. A **81**, 013404 (2010); J. S. Douglas and K. Burnett, Phys. Rev. A **84**, 033637 (2011).

[8] I. B. Mekhov, C. Maschler, and H. Ritsch, Nat. Phys. **3**, 319 (2007); Phys. Rev. Lett. **98**, 100402 (2007).
[9] P. Domokos and H. Ritsch, Phys. Rev. Lett. **89**, 253003 (2002).
[10] A. T. Black, H. W. Chan, and V. Vuletić, Phys. Rev. Lett. **91**, 203001 (2003).
[11] D. Nagy, G. Szirmai, and P. Domokos, Eur. Phys. J. D **48**, 127 (2008).
[12] J. Keeling, M. J. Bhaseen, and B. D. Simons, Phys. Rev. Lett. **105**, 043001 (2010).
[13] K. Baumann, C. Guerlin, F. Brennecke, and T. Esslinger, Nature (London) **464**, 1301 (2010).
[14] K. Baumann, R. Mottl, F. Brennecke, and T. Esslinger, Phys. Rev. Lett. **107**, 140402 (2011).
[15] J. K. Asbóth, P. Domokos, H. Ritsch, and A. Vukics, Phys. Rev. A **72**, 053417 (2005).
[16] S. Fernández-Vidal, G. De Chiara, J. Larson, and G. Morigi, Phys. Rev. A **81**, 043407 (2010).
[17] H. Habibian, S. Zippilli, and G. Morigi, Phys. Rev. A **84**, 033829 (2011).
[18] M. P. A. Fisher, P. B. Weichman, G. Grinstein, and D. S. Fisher, Phys. Rev. B **40**, 546 (1989).
[19] R. T. Scalettar, G. G. Batrouni, and G. T. Zimanyi, Phys. Rev. Lett. **66**, 3144 (1991); W. Krauth, N. Trivedi, and D. Ceperley, Phys. Rev. Lett. **67**, 2307 (1991).
[20] B. Damski, J. Zakrzewski, L. Santos, P. Zoller, and M. Lewenstein, Phys. Rev. Lett. **91**, 080403 (2003).
[21] B. Deissler, M. Zaccanti, G. Roati, C. D'Errico, M. Fattori, M. Modugno, G. Modugno, and M. Inguscio, Nat. Phys. **6**, 354 (2010).
[22] S. Gopalakrishnan, B. L. Lev, and P. M. Goldbart, Nat. Phys. **5**, 845 (2009).
[23] S. Gopalakrishnan, B. L. Lev, and P. M. Goldbart, Phys. Rev. Lett. **107**, 277201 (2011); P. Strack and S. Sachdev, Phys. Rev. Lett. **107**, 277202 (2011).
[24] C. Maschler and H. Ritsch, Phys. Rev. Lett. **95**, 260401 (2005).
[25] At finite temperature T, $\kappa_B T \ll \hbar/\Delta t$; see Ref. [16].
[26] S. Gupta, K. L. Moore, K. W. Murch, and D. M. Stamper-Kurn, Phys. Rev. Lett. **99**, 213601 (2007).
[27] We use a grand-canonical realization of the quantum Monte Carlo simulation [28], with which we identify the discontinuity of $\bar{n}$ at the border of the BG phase [Fig. 2(b)]. A conventional canonical simulation is used at the MI-SF border [29]. The blue points in Fig. 2(a) are determined when the jumps in the plots of $\bar{n}$ versus μ occur.
[28] P. Niyaz, R. T. Scalettar, C. Y. Fong, and G. G. Batrouni, Phys. Rev. B **50**, 362 (1994).
[29] G. G. Batrouni, R. T. Scalettar, and G. T. Zimanyi, Phys. Rev. Lett. **65**, 1765 (1990); G. G. Batrouni and R. T. Scalettar, Phys. Rev. B **46**, 9051 (1992).
[30] X. Deng, R. Citro, A. Minguzzi, and E. Orignac, Phys. Rev. A **78**, 013625 (2008).
[31] G. Roux, T. Barthel, I. P. McCulloch, C. Kollath, U. Schollwöck, and T. Giamarchi, Phys. Rev. A **78**, 023628 (2008).
[32] K. Sheshadri, H. R. Krishnamurthy, R. Pandit, and T. V. Ramakrishnan, Europhys. Lett. **22**, 257 (1993).
[33] L. Pollet, N. V. Prokof'ev, B. V. Svistunov, and M. Troyer, Phys. Rev. Lett. **103**, 140402 (2009).
[34] B. Damski and J. Zakrzewski, Phys. Rev. A **74**, 043609 (2006).
[35] M. Łącki, S. Paganelli, V. Ahufinger, A. Sanpera, and J. Zakrzewski, Phys. Rev. A **83**, 013605 (2011); S. Paganelli, M. Łącki, V. Ahufinger, J. Zakrzewski, and A. Sanpera, J. Low Temp. Phys. **165**, 227 (2011).
[36] K. J. Arnold, M. P. Baden, and M. D. Barrett, Phys. Rev. Lett. **109**, 153002 (2012).
[37] T. Volz, S. Dürr, S. Ernst, A. Marte, and G. Rempe, Phys. Rev. A **68**, 010702(R) (2003).
[38] P. Krüger, Z. Hadzibabic, and J. Dalibard, Phys. Rev. Lett. **99**, 040402 (2007).